First-principles LDA+U and GGA+U study of neptunium dioxide

Bao-Tian Wang,[1,2] Hongliang Shi,[2,3] Weidong Li,[1] and Ping Zhang[2,4,*]

[1]*Institute of Theoretical Physics and Department of Physics, Shanxi University, Taiyuan 030006, People's Republic of China*

[2]*LCP, Institute of Applied Physics and Computational Mathematics, Beijing 100088, People's Republic of China*

[3]*SKLSM, Institute of Semiconductors, Chinese Academy of Sciences, People's Republic of China*

[4]*Center for Applied Physics and Technology, Peking University, Beijing 100871, People's Republic of China*

(Received 2 November 2009; revised manuscript received 17 December 2009; published 20 January 2010)

We have performed a systematic first-principles investigation to calculate the electronic structures, mechanical properties, and phonon-dispersion curves of NpO_2. The local-density approximation+U and the generalized gradient approximation+U formalisms have been used to account for the strong on-site Coulomb repulsion among the localized Np 5f electrons. By choosing the Hubbard U parameter around 4 eV, the orbital occupancy characters of Np 5f and O 2p are in good agreement with recent experiments [A. Seibert, T. Gouder, and F. Huber, J. Nucl. Mater. **389**, 470 (2009)]. Comparing to our previous study of ThO_2, we note that stronger covalency exists in NpO_2 due to the more localization behavior of 5f electrons of Np in line with the localization-delocalization trend exhibited by the actinides series.

DOI: 10.1103/PhysRevB.81.045119 PACS number(s): 71.27.+a, 71.15.Mb, 71.20.−b, 63.20.dk

I. INTRODUCTION

Neptunium-based oxides have been extensively investigated by experiments[1–6] and theoretical calculations[7–10] due to the technological importance that neptunium is one of the important long-lived actinides which accumulate in high-level waste during the conventional nuclear fuel cycle. Among neptunium oxides, NpO_2 has attracted much more attention because of its more stable thermodynamical properties and interesting subtle noncollinear magnetic structure.[1–4] NpO_2 was reported to maintain stable under high temperature up to 1400 K.[1] Seibert *et al.* systematically studied the reaction of neptunium with molecular and atomic oxygen as well as the formation and stability of surface oxides; they reported that high neptunium oxides can only exist as surface phases not as stable bulk phases.[6] As for the electronic structures of actinide dioxides (AO_2), taking (A=U, Np, or Pu) O_2 for example, the 5f orbitals are partially occupied, accompanying the competition between the quantum process of localization and delocalization of A 5f electrons, which leads to many complex behaviors. This also makes the accurate description of electronic structure of AnO_2 series difficult to be achieved.

Conventional density-functional theory (DFT) that applies the local-density approximation (LDA) or generalized gradient approximation (GGA) underestimates the strong on-site Coulomb repulsion of the 5f electrons and, consequently, describes actinide dioxides as incorrect ferromagnetic (FM) metals instead of antiferromagnetic (AFM) Mott insulators. One more promising way to improve the drawback is LDA+U or GGA+U approach, in which the underestimation of the strong intra-atomic Coulomb interaction is corrected by the Hubbard U parameter. Recently, the electronic structures, mechanical properties, and high-pressure behaviors of UO_2 and PuO_2 have been correctly reproduced using LDA+U or GGA+U calculations.[8,11–15] The insulator character of NpO_2 is established by the experiments.[6,16] However, to our knowledge, a systematical theoretical investigation of electronic structure and mechanical properties for NpO_2 is still lacking. Consequently, based on the good performance of LDA/GGA+U approaches in describing the electronic structure of the strong-correlation systems, we carried out the present study of NpO_2.

In present study, the lattice parameter, electronic structure, mechanical features, and thermodynamic properties of NpO_2 are calculated by employing the LDA+U and GGA+U schemes due to Dudarev *et al.*[17] We discuss how the choice of U as well as the choice of exchange-correlation potential, i.e., the LDA or the GGA, affect those properties. Our results show that the pure LDA or GGA fails to give the accurate lattice parameter and correct electronic structure, while the LDA+U and GGA+U schemes can effectively remedy these failures. The rest of this paper is arranged as follows. In Sec. II, the computational method is briefly described. In Sec. III, we present and discuss our results. In Sec. IV, we summarize the conclusions of this work.

II. COMPUTATIONAL METHODS

Our total-energy calculations are carried out by employing the plane-wave basis pseudopotential method as implemented in Vienna *ab initio* simulation package (VASP).[18] The exchange and correlation effects are described by the DFT within LDA and GGA.[19,20] The projected augmented wave (PAW) method of Blöchl[21] is implemented in VASP with the frozen-core approximation. Electron wave function is expanded in plane waves up to a cutoff energy of 500 eV and all atoms are fully relaxed until the Hellmann-Feynman forces become less than 0.02 eV/Å. A $9\times9\times9$ Monkhorst-Pack[22] k-point mesh in the full wedge of the Brillouin zone is used for fluorite NpO_2. The neptunium $6s^27s^26p^66d^25f^3$ and oxygen $2s^22p^4$ electrons are treated as valence electrons. The strong on-site Coulomb repulsion among the localized Np 5f electrons is described by using the formalism formulated by Dudarev *et al.*[17] In this scheme, the total LDA (GGA) energy functional is of the form

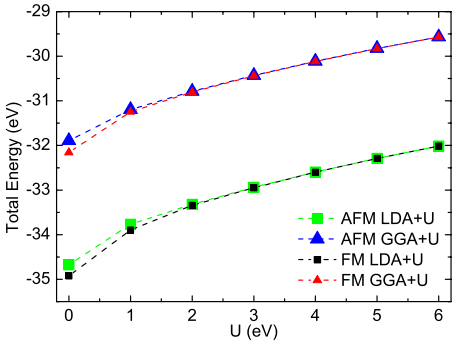

FIG. 1. (Color online) Dependences of the total energies (per formula unit) on U for FM and AFM NpO_2.

$$E_{\mathrm{LDA(GGA)}+U} = E_{\mathrm{LDA(GGA)}} + \frac{U-J}{2}\sum_{\sigma}[\mathrm{Tr}\,\rho^{\sigma} - \mathrm{Tr}(\rho^{\sigma}\rho^{\sigma})], \qquad (1)$$

where ρ^{σ} is the density matrix of f states with spin σ, while U and J are the spherically averaged screened Coulomb energy and the exchange energy, respectively. In this paper, the Coulomb U is treated as a variable, while the exchange energy is set to be a constant J=0.6 eV. This value of J is in the ball park of the commonly accepted one for Np.[8] Since only the difference between U and J is significant,[17] thus we will henceforth label them as one single parameter, for simplicity labeled as U, while keeping in mind that the nonzero J has been used during calculations.

Both spin-unpolarized and spin-polarized calculations are performed in this study. Compared to FM and AFM phases, the nonmagnetic (NM) phase is not energetically favorable both in the LDA+U and GGA+U formalisms. Therefore, the results of NM are not presented in the following. The dependence of the total energy (per formula unit at respective optimum geometries) on U for both FM and AFM phases within the LDA+U and GGA+U formalisms is shown in Fig. 1. On the whole, the total energy of FM phase is lower than that of AFM phase either in LDA+U scheme or GGA +U scheme. However, as shown in Fig. 1, it is clear that the difference can be negligible, especially as the increasing of the U parameter. The total-energy differences ($E_{\mathrm{FM}}-E_{\mathrm{AFM}}$) within the LDA+$U$ at U=4 and 6 eV are −0.005 eV, which is close to previous calculation[8] (−0.004 eV for U =4.25 eV), and −0.002 eV, respectively. We stress that our approach does not include the spin-orbit coupling (SOC); a detailed explanation on this issue can be found in Ref. 23. Both FM and AFM results will be presented in the following analysis.

In this study, the theoretical equilibrium volume, bulk modulus B, and pressure derivative of the bulk modulus B' are obtained by fitting the third-order Birch-Murnaghan equation of state (EOS).[24] The elastic constants, various moduli, and Poisson's ratio υ are calculated using the same method of our previous work.[25] Note that the bulk modulus B obtained by these two approaches is in good agreement, indicating that our calculations are self-consistent.

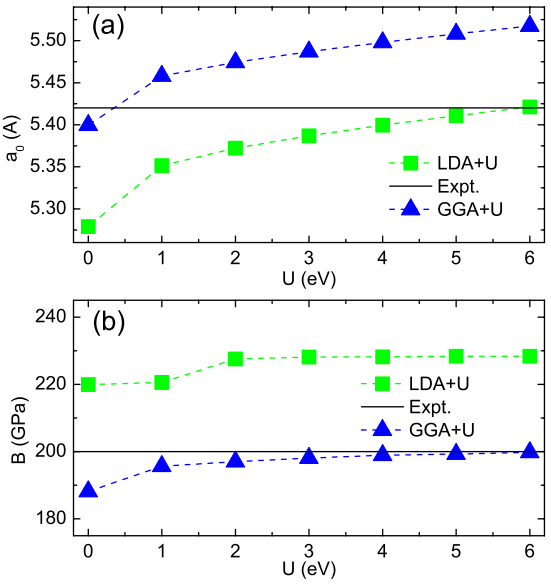

FIG. 2. (Color online) Dependences of the (a) lattice parameter and (b) bulk modulus on U for AFM NpO_2.

III. RESULTS

A. Atomic and electronic structures of NpO_2

At room-temperature and zero-pressure conditions, the stoichiometric neptunium dioxide crystallizes in a CaF_2-like ionic structure with space group $Fm\bar{3}m$ (No. 225), which is the stable structure of all actinide dioxides. Its cubic unit cell (defined by the lattice parameter a_0) is composed of four NpO_2 formula units with the neptunium atoms and the oxygen atoms in 4a and 8c sites, respectively. At higher pressure, ~33 GPa experimentally, Benedict *et al.*[3] reported that NpO_2 undergoes a phase transition to an orthorhombic $Cmcm$ (No. 63) structure. In this study, we only focus our sight on the $Fm\bar{3}m$ NpO_2.

The present optimized lattice constant a_0 and bulk modulus B, obtained by fitting the EOS for AFM NpO_2, are presented in Fig. 2. For comparison, the experimental values of a_0 (Ref. 2) and B (Ref. 3) are also shown. Note that the experimental value of a_0(5.42 Å) (Ref. 2) is the fitted value at 0 K rather than at ambient condition. In the overall view, the dependence of the lattice parameter a_0 of NpO_2 on U is similar to our previous study of PuO_2.[13] For the pure DFT calculations (U=0), as shown in Fig. 2(a), both LDA and GGA underestimate the lattice parameter with respect to the experimental value. This trend is more evident for LDA due to its overbinding character. After turning on the Hubbard U, for the LDA+U approach, although the lattice parameter is still underestimated in a wide range of U, the calculated a_0 improves upon the pure LDA by steadily increasing its amplitude with U. Actually, at a typical value U=4 eV, the LDA+U gives a_0=5.40 Å which is very close to the experimental value. On the other hand, the GGA+U enlarges the underbinding effect with increasing Hubbard U. As a comparison, at U=4 eV, the GGA+U gives a_0=5.50 Å. Totally speaking, both the LDA+U and GGA+U results of the lattice parameter for the NpO_2 AFM phase are comparable to

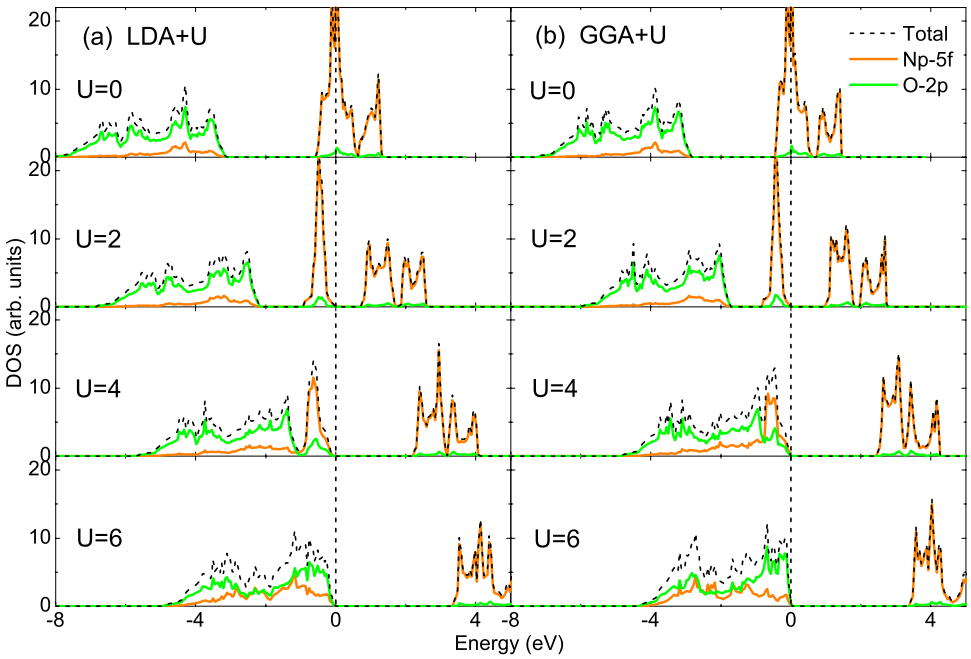

FIG. 3. (Color online) The total DOS for the NpO_2 AFM phase computed in the (a) LDA+U and (b) GGA+U formalisms with four selective values of U. The projected DOSs for the Np 5f and O 2p orbitals are also shown. The Fermi energy level is set at zero.

the experimental value at U around 4 eV. We have also calculated the equilibrium lattice parameter for the FM phase for NpO_2. The tendency of a_0 with U is similar to that of the AFM phase. Note that the screened Coulomb hybrid functional[7] and self-interaction-corrected local spin-density (SIC-LSD) (Ref. 10) calculations predicted the lattice parameter to be 5.42 and 5.46 Å, respectively.

As for the dependence of bulk modulus B of AFM NpO_2 on U shown in Fig. 2(b), it is clear that the LDA results (220–228 GPa) are always higher than the GGA results (188–200 GPa), which is due to the above-mentioned overbinding effect of the LDA approach. At a typical value U=4 eV, the LDA+U and GGA+U give B=228 and 199 GPa, respectively. Apparently, the GGA+U approach with increasing U gives more close values to the experimental data of B=200 GPa.[3] Note that the recent LDA+U (Ref. 8) and SIC-LSD (Ref. 10) calculations predicted the bulk modulus to be 228 and 217 GPa for AFM NpO_2, respectively. Overall, comparing to the experimental data and recent theoretical results, the accuracy of our atomic-structure prediction for AFM NpO_2 is quite satisfactory by tuning the effective Hubbard parameter U in a range of 3–4 eV within the LDA/GGA+U approaches, which supplies the safeguard for our following study of electronic structure and mechanical properties of NpO_2.

Almost all the macroscopical properties of materials, such as hardness, elasticity, and conductivity, originate from their electronic structure properties as well as chemical bonding nature. Therefore, a correct description of electronic structure is necessary for further investigating these properties. In the following, we will show the dramatic improvement brought by the LDA/GGA+U schemes compared to the pure ones as describing the electronic structure properties of NpO_2. The total density of states (DOS) as well as the projected DOS for the Np 5f and O 2p orbitals at four selective values of U within LDA/GGA+U formalisms are shown in Fig. 3. Without accounting for the on-site Coulomb repulsion (U=0), one can see that both LDA and GGA methods predict an incorrect metallic ground state with nonzero occupation of Np 5f states at E_F. After switching on U, as shown in Fig. 3, the Np 5f bands begin to split at E_F and tend to open a Mott-type gap E_g. The amplitude of this insulating gap increases with increasing U (see Fig. 4). Overall, the LDA+U and GGA+U give an equivalent description of the one-electron behaviors in a wide range of U. At a typical value U=4 eV, one can see from Fig. 3 that the occupied DOS near the Fermi level is featured by the three well-resolved peaks. The narrow one near −1.0 eV is principally Np 5f in character, while the other two broad peaks, respectively, near −2.0 and −4.0 eV are mostly O 2p. These well-separated orbital peaks have been observed in the recent ultraviolet photoelectron spectroscopy (UPS) measurement.[6] In addition, The width of the Np 5f valence band is 1 eV, consistent with the hybrid functional calculation[7] and experimental data.[6] The O 2p valence-band width is of 4.5 eV, also in accord with the experimental data (4 eV) and previous hybrid functional result (4.5 eV). The Mott gap that opened at

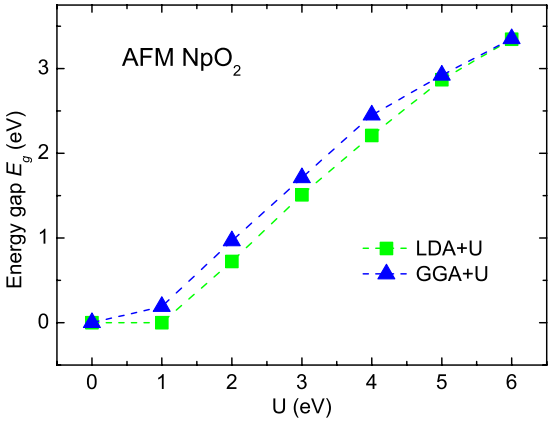

FIG. 4. (Color online) The LDA/GGA+U insulating band gap for the AFM NpO_2.

TABLE I. Calculated elastic constants, various moduli, pressure derivative of the bulk modulus B', Poisson's ratio υ, spin moments ($\mu_{mag.}$), and insulating band gap (E_g) for $Fm\bar{3}m$ NpO_2 at 0 GPa. For comparison, experimental values from Ref. 3 are also listed.

Magnetism	Method	C_{11} (GPa)	C_{12} (GPa)	C_{44} (GPa)	B (GPa)	B'	G (GPa)	E (GPa)	υ	$\mu_{mag.}$ (μ_B)	E_g (eV)
AFM	LDA+U(U=0)	405.1	128.8	78.9	221	4.1	98.9	258.2	0.305	2.678	0.0
	LDA+U(U=4)	399.5	145.5	72.9	230	4.5	91.2	241.6	0.325	3.074	2.2
	GGA+U(U=0)	358.7	105.2	53.5	190	4.2	76.2	201.7	0.323	2.903	0.0
	GGA+U(U=4)	363.6	118.8	57.4	200	4.3	78.1	207.5	0.327	3.092	2.4
	Expt.				200	3.8					
FM	LDA+U(U=0)	415.0	148.7	79.3	237	4.5	97.7	257.8	0.319	3.054	0.0
	LDA+U(U=4)	403.6	143.4	73.7	230	4.2	92.7	245.2	0.323	3.090	2.1
	GGA+U(U=0)	372.7	116.8	70.9	202	4.4	90.0	235.1	0.306	3.104	0.0
	GGA+U(U=4)	365.8	117.8	57.5	200	4.5	78.6	208.6	0.327	3.103	2.4

U=4 eV is of 2.2 (2.4) eV within the LDA(GGA)+U scheme (see Table I). Previous hybrid functional calculations result in a larger E_g by ~0.8 eV.[7] The calculated amplitude of local spin moment is ~3.1μ_B (per Np atom) in both AFM and FM phases and within the two DFT+U schemes. On the whole, although the pure LDA and GGA fail to depict the electronic structure, especially the insulating nature and the occupied-state character of NpO_2, our present results show that by tuning the effective Hubbard parameter in a reasonable range, the LDA/GGA+U approaches can prominently improve upon the pure LDA/GGA calculations and, thus, can provide a satisfactory qualitative electronic structure description comparable to the experiments. By further increasing U to 6 eV, one can see that the peak near −1.0 eV becomes weak and is mostly O 2p. Meanwhile, there develops a prominent hybridization between Np 5f and O 2p orbitals. This picture of DOS is no longer valid since the peak near the valence-band maximum has been experimentally verified[6] to be due to the Np 5f contribution. Thus, the overestimation of U will compel Np 5f orbitals to be even more localized, resulting in their unphysical alignment with the O 2p orbitals.

In order to understand the chemical bonding nature of ground state NpO_2, we plot in Fig. 5 the valence charge-density map of the $(1\bar{1}0)$ plane. Evidently, the charge densities around Np and O ions are all near spherical distribution with slightly deformed toward the direction to their nearest-neighboring atoms. Moreover, the charge density around Np and O ions is high while there are almost no remaining valence charges in the large octahedral-hole interstitial region, clearly indicating ionization of neptunium and oxygen ions and significant insulating behavior of AFM NpO_2. We have also plotted the line charge-density distribution along the nearest Np-O bond (not shown) and find that the minimum value of charge density is 0.51 $e/Å^3$. The distance between this minimum point and Np ion is 1.29 Å. Thus, the ionic radius of Np in NpO_2 can be defined as r_{Np}=1.29 Å, which is bigger than the Shannon ionic radius of Np (0.98 Å).[26] After subtracting r_{Np} from the Np-O bond length (2.34 Å), the oxygen ionic radius r_O=1.05 Å, which is smaller than the Shannon ionic radius of O (1.38 Å),[26] can be obtained. The corresponding valency of Np and O in NpO_2 can be estimated by calculating the valence charges within the spheres of ionic radii. After integration, we find 11.386 electrons around Np and 6.233 electrons around O. Therefore, the valency of Np and O can be represented as $Np^{3.614+}$ and $O^{0.233-}$, respectively. This inequivalent valency for oxygen and metal ions is to some extent similar to that happened in metal hydrides.[27] We note that the ionicity of Np-O bond is relatively weaker when compared to the Th-O bond in ThO_2.[25] On the other hand, the Np-O bond has stronger covalency than the Th-O bond due to that the minimum value 0.51 $e/Å^3$ of charge density along the Np-O bond in which NpO_2 is prominently larger than that along the Th-O bond (0.45 $e/Å^3$) in ThO_2.[25] This finding is consistent with the fact that the 5f orbitals are more localized in the former in line with the localization-delocalization trend demonstrated by the actinide series. Through analyzing the orbital-resolved partial densities of states (PDOS) for the AFM NpO_2, we find that the ionicity of the Np-O bond can be attributed to the charge transfer from Np 6d and 5f states to O 2p states and the covalent bonding of the Np-O bond is associated with the hybridization of Np 5f and O 2p states.[8] Overall, the Np-O bond can be described as a mixture of covalent and ionic components.

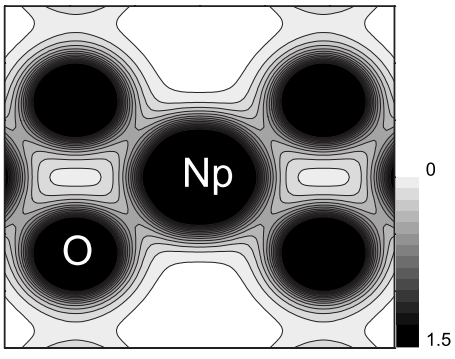

FIG. 5. Valence charge density of AFM NpO_2 in $(1\bar{1}0)$ plane computed in the LDA+U formalisms with U=4 eV. Contour lines are drawn from 0.0 to 1.5 at 0.1 $e/Å^3$ intervals.

B. Mechanical properties of NpO_2

Our calculated elastic constants, various moduli, pressure derivative of the bulk modulus B', and Poisson's ratio υ for $Fm\bar{3}m$ NpO_2 at 0 GPa are collected in Table I. Here, the moduli and Poisson's ratio are deduced from the calculated elastic constants using the same scheme as that in our previous study on isostructural ThO_2.[25] Each derived bulk modulus B turns out to be very close to that obtained by EOS fitting. This indicates that our calculations are consistent and reliable. At a typical value of $U=4$ eV, LDA+U gives bulk modulus of 230 GPa for both AFM and FM NpO_2, while GGA+U gives 200 GPa. Obviously, GGA+U approach gives closer value than LDA+U with respect to the experimental value. Overall, the bulk modulus of NpO_2 is bigger than that of ThO_2.[25] This originates from relative higher valence electron density and shorter bond distances of NpO_2 than those of ThO_2.

In addition, the hardness of NpO_2 is investigated by using the approach raised by Simunek and Vackar.[28] In the case of two atoms 1 and 2 forming one bond of strength s_{12} in a unit cell of volume Ω, the expression for hardness has the form[28]

$$H = (C/\Omega) b_{12} s_{12} e^{-\sigma f_2}, \tag{2}$$

where

$$s_{12} = \sqrt{(e_1 e_2)}/(n_1 n_2 d_{12}), \quad e_i = Z_i/r_i \tag{3}$$

and

$$f_2 = \left(\frac{e_1 - e_2}{e_1 + e_2}\right)^2 = 1 - [\sqrt{(e_1 e_2)}/(e_1 + e_2)]^2 \tag{4}$$

are the strength and ionicity of the chemical bond, respectively, and d_{12} is the interatomic distance; $C=1550$ and $\sigma=4$ are constants. The radius r_i is chosen to make sure that the sphere centered at atoms i in a crystal contains exactly the valence electronic charge Z_i. For fluorite structure NpO_2, $b_{12}=32$ counts the interatomic bonds between atoms Np (1) and O (2) in the unit cell, $n_1=8$ and $n_2=4$ are coordination numbers of atom Np and O, respectively, $r_1=1.715$ (Å) and $r_2=1.000$ (Å) are the atomic radii for Np and O atoms, respectively, $Z_1=15$ and $Z_2=6$ are valence charge for Np and O atoms, respectively, $d_{12}=2.34$ (Å) is the interatomic distance, and $\Omega=157.42$ (Å^3) is the volume of unit cell. Using Eqs. (2)–(4), we obtain $s_{12}=0.0967$ and $f_2=0.0347$. The hardness of NpO_2 at its ground-state fluorite structure is thus given by $H=26.5$ (GPa). This indicates that the fluorite NpO_2 is a hard material and approaches to a superhard material (hardness >40 GPa). The high hardness of this crystal can be understood from the dense crystal structure, which results in high valence electron density and short bond distances. We notice that the hardness of NpO_2 is higher than that of ThO_2 (22.4 GPa).[25] This also can be attributed to the higher electron density and shorter bond distance of NpO_2 compared to ThO_2.

C. Phonon dispersion curve of NpO_2

Before phonon-dispersion calculation, we have calculated the Born effective charges and dielectric constants of NpO_2 because of their critical importance to correct the LO-TO splitting. The Born effective charge Z^* is a measurement of the change in electronic polarization due to the ionic displacements. The form of Z^* for a particular atom depends on the atomic position symmetry. For fluorite NpO_2, the effective charge tensors for both Np and O that occupy the $4a$ and $8c$ Wyckhoff positions, respectively, are isotropic. After calculation, the Born effective charges of Np and O ions for AFM (FM) NpO_2 are found to be $Z^*_{Ce}=5.24(5.26)$ and $Z^*_O=-2.62(-2.63)$, respectively, within LDA+U formalism with the choice of $U=4.0$ eV. In addition, the macroscopic static dielectric tensor is also isotropic and our computed value of dielectric constant ε_∞ is 5.58 for the AFM phase and 5.64 for the FM phase.

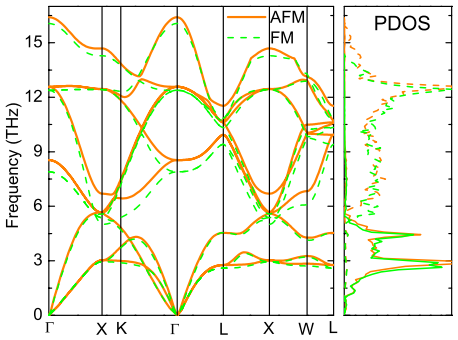

FIG. 6. (Color online) Calculated phonon-dispersion curves (left panel) and corresponding PDOS (right panel) for NpO_2. Both the AFM and FM results are calculated within LDA+U formalism with $U=4$ eV. In right panel, the orange and green lines stand for AFM and FM results, respectively, while solid and dashed lines are used to distinguish the PDOS of Np and O.

Employing the Hellmann-Feynman theorem and the direct method,[29] we have calculated the phonon curves along some high-symmetry directions in the Brillouin zone (BZ) together with the phonon density of states. For the phonon-dispersion calculation, we use the $2\times2\times2$ fcc supercell containing 96 atoms and the $4\times4\times4$ Monkhorst-Pack k-point mesh for the BZ integration. In order to calculate the Hellmann-Feynman forces, we displace four atoms (two Np and two O atoms) from their equilibrium positions and the amplitude of all the displacements is 0.03 Å. The calculated phonon-dispersion curves along the $\Gamma-X-K-\Gamma-L-X-W-L$ directions are displayed in Fig. 6 for both FM and AFM phases of NpO_2.

To our knowledge, no experimental phonon frequency results have been published for NpO_2. In the CaF_2-structure primitive cell, there are only three atoms (one Np and two O atoms). Therefore, nine phonon modes exist in the dispersion relations. One can see that the gap between the optic modes and the acoustic branches is not so evident. But the LO-TO splitting at Γ point is very significant since the inclusion of polarization effects. Due to the fact that neptunium is heavier than oxygen atom, the vibration frequency of neptunium atom is lower than that of oxygen atom. Therefore, the phonon density of states for NpO_2 can be viewed as two parts. One is the part lower than 5.7 (5.0) THz for AFM (FM) NpO_2 where the main contribution comes from the neptunium sublattice, while the other part higher than 5.7 (5.0)

THz is dominated by the dynamics of the light oxygen atoms. In addition, one can see from Fig. 6 that the difference in the phonon dispersion between the FM and AFM phases of NpO_2 is negligible in most regions of the BZ, except for one TO branch which is a little lower for the FM phase than for the AFM phase.

IV. CONCLUSION

In conclusion, we have studied the structural, electronic, mechanical, and thermodynamic properties of NpO_2 within the LDA+U and GGA+U formalisms. The atomic structure, including lattice parameters and bulk modulus, and the one-electron behaviors of 5f state have been systematically investigated as a function of the effective on-site Coulomb repulsion parameter U. By choosing the Hubbard U parameter around 4 eV within the LDA/GGA+U approaches, most of our calculated results are in good agreement with the experiments. Based on this, we have further investigated the electronic structures of NpO_2 and the Np-O bond nature. The insulating ground state can be well reproduced and the Np-O bond is found to be of a mixture of both the ionic and covalent characters. As for the mechanical property, we find that GGA+U approach gives closer value of bulk modulus than LDA+U with respect to the experimental value and the hardness of NpO_2 is calculated to be 26.5 GPa. For the thermodynamic analysis, the Born effective charges and dielectric constants as well as the phonon-dispersion curves have also been presented.

ACKNOWLEDGMENTS

This work was supported by the Foundations for Development of Science and Technology of China Academy of Engineering Physics under Grant No. 2009B0301037 and NCET of the Ministry of Education of China (Grant No. NCET-08-0883).

*Author to whom correspondence should be addressed; zhang_ping@iapcm.ac.cn

[1] H. Serizawa, Y. Arai, and K. Nakajima, J. Chem. Thermodyn. **33**, 615 (2001).
[2] T. Yamashita, N. Nitani, T. Tsuji, and H. Inagaki, J. Nucl. Mater. **247**, 90 (1997).
[3] U. Benedict, S. Dabos, C. Dufour, and J. C. Spirlet, J. Less-Common Met. **121**, 461 (1986).
[4] P. Santini, S. Carretta, G. Amoretti, R. Caciuffo, N. Magnani, and G. H. Lander, Rev. Mod. Phys. **81**, 807 (2009).
[5] T. Nishi, A. Itoh, M. Takano, M. Numata, M. Akabori, Y. Arai, and K. Minato, J. Nucl. Mater. **376**, 78 (2008).
[6] A. Seibert, T. Gouder, and F. Huber, J. Nucl. Mater. **389**, 470 (2009).
[7] I. D. Prodan, G. E. Scuseria, and R. L. Martin, Phys. Rev. B **76**, 033101 (2007).
[8] D. A. Andersson, J. Lezama, B. P. Uberuaga, C. Deo, and S. D. Conradson, Phys. Rev. B **79**, 024110 (2009).
[9] K. Kurosaki, M. Imamura, I. Sato, T. Namekawa, M. Uno, and S. Yamanaka, J. Alloys Compd. **387**, 9 (2005).
[10] L. Petit, A. Svane, Z. Szotek, W. M. Temmerman, and G. M. Stocks, arXiv:0908.1806 (unpublished).
[11] H. Y. Geng, Y. Chen, Y. Kaneta, and M. Kinoshita, Phys. Rev. B **75**, 054111 (2007).
[12] S. L. Dudarev, D. N. Manh, and A. P. Sutton, Philos. Mag. B **75**, 613 (1997).
[13] B. Sun, P. Zhang, and X.-G. Zhao, J. Chem. Phys. **128**, 084705 (2008).
[14] B. Sun and P. Zhang, Chin. Phys. B **17**, 1364 (2008).
[15] G. Jomard, B. Amadon, F. Bottin, and M. Torrent, Phys. Rev. B **78**, 075125 (2008).
[16] B. W. Veal, D. J. Lam, and H. R. Hoekstra, Phys. Rev. B **15**, 2929 (1977).
[17] S. L. Dudarev, G. A. Botton, S. Y. Savrasov, C. J. Humphreys, and A. P. Sutton, Phys. Rev. B **57**, 1505 (1998).
[18] G. Kresse and J. Furthmüller, Phys. Rev. B **54**, 11169 (1996).
[19] W. Kohn and L. J. Sham, Phys. Rev. **140**, A1133 (1965).
[20] J. P. Perdew, K. Burke, and Y. Wang, Phys. Rev. B **54**, 16533 (1996).
[21] P. E. Blöchl, Phys. Rev. B **50**, 17953 (1994).
[22] H. J. Monkhorst and J. D. Pack, Phys. Rev. B **13**, 5188 (1976).
[23] I. D. Prodan, G. E. Scuseria, and R. L. Martin, Phys. Rev. B **73**, 045104 (2006).
[24] F. Birch, Phys. Rev. **71**, 809 (1947).
[25] B. Wang, H. Shi, W. Li, and P. Zhang, arXiv:0908.3558 (unpublished).
[26] R. D. Shannon, Acta Crystallogr., Sect. A: Cryst. Phys., Diffr., Theor. Gen. Crystallogr. **32**, 751 (1976).
[27] T. Noritake, M. Aoki, S. Towata, Y. Seno, Y. Hirose, E. Nishibori, M. Takata, and M. Sakata, Appl. Phys. Lett. **81**, 2008 (2002).
[28] A. Simunek and J. Vackar, Phys. Rev. Lett. **96**, 085501 (2006).
[29] K. Parlinski, Z. Q. Li, and Y. Kawazoe, Phys. Rev. Lett. **78**, 4063 (1997).